Detection of Diabetic Symptoms in Retina Images Using Analog Algorithms

Daniela Matei, Radu Matei

***Abstract*—**In this paper a class of analog algorithms based on the concept of Cellular Neural Network (CNN) is applied in some processing operations of some important medical images, namely retina images, for detecting various symptoms connected with diabetic retinopathy. Some specific processing tasks like morphological operations, linear filtering and thresholding are proposed, the corresponding template values are given and simulations on real retina images are provided.

***Keywords*—**Diabetic retinopathy, pathology detection, cellular neural networks, analog algorithms.

I. Introduction

DIABETIC neuropathy is one of the serious complications caused by diabetes, causing pathological changes in the retina, which is the most important tissue of the eye, and therefore affects vision [1], [2]. There may exist different kinds of abnormal lesions caused by diabetic retinopathy, the most frequent being microaneurysm, hard exudate, soft exudate, hemorrhage, and neovascularization. All these pathologies have specific characteristics and are important in the clinical assessment of this disorder. Microaneurysms are the earliest clinically detectable lesions. Neovascularization is the most serious abnormality type in diabetic retinopathy and consists in the formation of new blood vessels that are weak and can therefore easily break, causing hemorrhages which appear as dark irregular spots on the retina. Hard exudates are lipid formations leaked from weakened vessels and usually appear in clusters. Soft exudates (micro-infarctions) appear due to obstruction of retinal arterioles. Both hard and soft exudates lesions appear brighter than the neighborhood.

Some of the main issues regarding medical image processing are image enhancement, feature extraction, classification etc. employing analog and/or digital techniques. For some applications requiring image processing in real time, fast dedicated digital processors are used. When some fast pre-processing stages are required, a noteworthy alternative might be an analog, parallel array processor, using for instance the concept of cellular neural networks (CNNs) [3]-[7]. These systems consist of large, regular arrays of dynamic processing elements (cells) which are identical and identically connected together, and their global behavior can be controlled by *template* parameters, adjusted digitally [6]. This parallel processing leads to a large equivalent computing power. For various processing operations, the template parameters have to be determined. Several applications of CNNs in biomedical imaging have been proposed [8]-[11].

Cellular Neural Networks can perform both linear and nonlinear image processing tasks, such as filtering, thresholding, various mathematical morphology operations, edge detection, corner detection etc. The range of such processing tasks is quite large and due to its parallel architecture, the CNN is able to operate very fast, the processing being practically done in real time [6].

As a preprocessing step in a possible application envisaging an automatic diagnosis or assessment of such diabetic symptoms, it would be desirable to separate, using a sequence of simple processing tasks, the imagistic details representing different lesions or abnormalities, as those aforementioned. A standard CNN of size $N \times N$ is described by the non-linear system of state-equations:

$$C\frac{dx_{ij}(t)}{dt} = -\frac{1}{R_x}x_{ij}(t) + \sum_{k,l} A_{ijkl}y_{kl}(t) + \sum_{k,l} B_{ijkl}u_{kl} + I \qquad (1)$$

where $1 \le i, j \le N$ and the output is a piece-wise linear function of the current state:

$$y_{ij}(t) = 0.5\left(\left|x_{ij}(t)+1\right| - \left|x_{ij}(t)-1\right|\right) \qquad (2)$$

The coefficients A_{kl}, B_{kl} in the convolution sums in (1) correspond to the feedback and control *templates* A and B.

II. Detection of Pathological Elements on Retina Images Using CNN Analog Algorithms

In this main section of the paper we propose some pre-processing algorithms which can be applied to retina images, in order to detect the presence of specific abnormalities characteristic of diabetic retinopathy, mentioned in the introduction. We will consider the grayscale image of a retina presenting moderate symptoms of diabetic retinopathy, namely spots and blood vessels; the fine capillaries are clearly visible and the image resolution is high enough (500×600)..

A. Detection of Blood Vessels and Hemorrhages Using Thresholding and Morphological Operations

In order to assess the presence of retinopathy symptoms, the

D.Matei is with the University of Medicine and Pharmacy, Iasi, Romania, Faculty of Biomedical Engineering (e-mail: dvm2202@yahoo.com).

R.Matei is with the Technical University of Iasi, Romania, Faculty of Electronics and Telecommunications (phone: +40 232 213737; fax: +40 232 217720; e-mail: rmatei@etc.tuiasi.ro).

blood vessel distribution (referred to as *vessel map*) must be separated from other details. The basic retina image which was processed is shown in Fig.1(a). It is a typical image presenting retinopathy symptoms in a moderate degree, namely neovascularization (a fine network of capillaries), dark compact spots representing hemorrhages and more diffuse white spots indicating the presence of exudates. On a grayscale retina image, hemorrhages spots will appear in a darker level of gray. Taking into account the size and compactness of the hemorrhage spots, they can be separated using two distinct morphological processing steps. Morphological operations can be performed on binary images using CNN operators. Thus the preliminary step is to obtain a convenient binary image from the original retina image through a thresholding task using a properly chosen threshold value. This binary image contains all visible blood vessels and possibly hemorrhage spots. The threshold value is chosen such that image segmentation is optimal. The templates are:

$$A=\begin{bmatrix}0&0&0\\0&2&0\\0&0&0\end{bmatrix};\ B=\begin{bmatrix}0&0&0\\0&0&0\\0&0&0\end{bmatrix};\ I=th$$

where the threshold value is *th*, with $-1<th<1$.

The next step is the detection itself. First, an erosion operation can be performed with an usually circular structural element. In a given number of successive steps, all of the image details (blood vessels etc.) are removed through erosion, while the largest elements like the compact spots representing hemorrhages are eroded but they still remain on the binary image. The number of erosion operations depends on the binary image details; if the relevant hemorrhage spots are consistent compared to the rest of image details, fewer erosion steps will be necessary until the latter are removed. The erosion may continue until most of smaller objects decrease to a few pixels, when they can be removed using another morphological operation, for instance *small object killing*, which removes them without affecting the larger objects of interest. Once the hemorrhage spots are detected through erosion, they can be approximately reconstructed using the reverse operation, namely dilation, using the same structural element. This succession of tasks is shown in Fig.1.

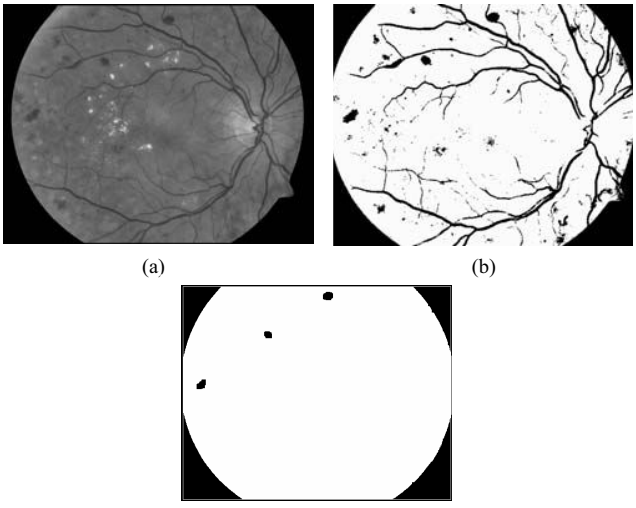

(a) (b) (c)

Fig. 1. (a) Original retina image; (b) binary image after thresholding; (c) detected hemorrhages

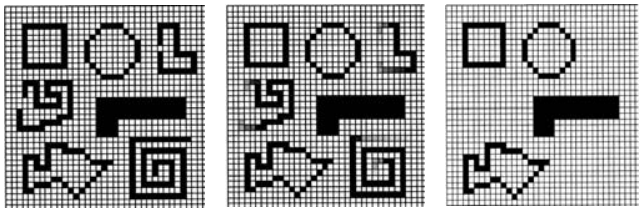

Input image Intermediate image Output image

Fig. 2. Deletion of open curves and detection of closed curves

Angiography images (obtained by previously injecting a contrast substance) are more convenient for hemorrhage detection since on the grayscale retina image the blood vessels appear in a light gray level, while the hemorrhage spots appear dark; therefore, they can be easily separated by thresholding. An object skeletonization operation may be also applied, which erodes all objects from the binary image without removing them; as a result, the blood vessels will appear as one-pixel thin curves. Therefore, skeletonization preserves the basic information about the retina vascular structure. The hemorrhage spots are also eroded, becoming thin structures which can be easily removed. The skeletonization operation can be conveniently implemented on a CNN universal machine as a subroutine which applies successively 8 control templates size 3×3. The feedback template A is also of size 3×3 and is zero everywhere except the central element which is equal to one. The first two control templates and the corresponding bias current values are [5]:

$$B_1=\begin{bmatrix}1&1&0\\1&5&-1\\0&-1&0\end{bmatrix},\ I_1=-1;\ B_2=\begin{bmatrix}2&2&2\\0&9&0\\-1&-2&-1\end{bmatrix},\ I_1=-2$$

Other useful operations proposed by the authors, which can be applied on the skeletonized image are:

1. Erasing thin lines from a binary image [14]. The templates and the bias current value are:

$$A=\begin{bmatrix}2&2&2\\2&8&2\\2&2&2\end{bmatrix};\ B=\begin{bmatrix}0&0&0\\0&0&0\\0&0&0\end{bmatrix};\ I=-2$$

The binary image is loaded as initial state: **X(0) = P** and the input is arbitrary or as default: U(t)=0.

2. Detection of closed curves: Detects the one-pixel thick closed curves and deletes the open curves from a binary image [14]. The binary image **P** is applied at the system input and also loaded as initial state: **U(t) = P**, **X(0) = P**; the templates and bias curent for this task are:

$$A=\begin{bmatrix}6&6&6\\6&9&6\\6&6&6\end{bmatrix};\ B=\begin{bmatrix}-3&-3&-3\\-3&9&-3\\-3&-3&-3\end{bmatrix};\ I=-4.5$$

The final image will contain all closed curves present in the initial image **P**.

B. Image Pre-processing by Gaussian Filtering

In biomedical imaging applications, image blurring is sometimes a pre-processing step, usually done using Gaussian low-pass filters. Although the design methods for Gaussian filters are well known, we briefly describe an efficient design method dedicated to CNN implementation, as follows. When CNNs are used as stable linear 2-D filters, the image **I** to be filtered is usually applied at the input (**U=I**) and the initial state is usually zero (**X=0**). The cells must not reach saturation during operation, which implies the restriction for the cell state: $|x_{ij}(t)|<1$, $i,j=1...N$. The linear CNN filter is described by the transfer function [4]:

$$H(\omega_1,\omega_2) = -B(\omega_1,\omega_2)/A(\omega_1,\omega_2) \quad (3)$$

where $A(\omega_1,\omega_2)$, $B(\omega_1,\omega_2)$ are the 2-D Discrete Space Fourier Transforms of templates *A, B*. A simple design method for 2D low-pass (LP) Gaussian filters is given in [12]:

$$G(\omega) = \exp\left(-\sigma^2\omega^2/2\right) \quad (4)$$

We can find a rational approximation of $G(\omega)$ using the variable change $\omega = \arccos(x) \Leftrightarrow x = \cos(\omega)$. For $\sigma = 1$, we get the first order Padé approximation:

$$G(\omega) = \exp\left(-\omega^2/2\right) \cong \left(a_0 + a_1\cdot\cos\omega\right)/\left(a_0 + a_1\cdot\cos\omega\right) \quad (5)$$

The -3dB bandwidth (*cut-off frequency*) can be found imposing the condition: $\exp\left(-\sigma^2\omega_C^2/2\right) = 1/\sqrt{2}$

$$\omega_C = \sqrt{2\ln\sqrt{2}}/\sigma = 0.833/\sigma \quad (6)$$

The numerator and denominator coefficients are: $B_1 = [0.5a_1 \quad a_0 \quad 0.5a_1]$, $A_1 = [0.5a_2 \quad 1 \quad 0.5a_2]$ $a_0 = 0.28116$, $a_1 = 0.27261$, $a_2 = -0.44625$. The exact and approximated characteristics are shown in Fig.2(a), being almost identical. However, we might need more selective low-pass filters, for larger values of σ. In this case, we get higher-order Padé approximations. Another way to obtain a more selective Gaussian characteristic is to consider $G(\omega)$ in (4) as an elementary or "kernel" function, and to apply it several times. This is equivalent to the Gaussian (for integer N):

$$G_N(\omega) = \left(G(\omega)\right)^N = \frac{(a_0 + a_1\cdot\cos\omega)^N}{(1 + a_2\cdot\cos\omega)^N} \quad (7)$$

For instance, taking $\sigma = 2$ (N=4), we get:

$$G_4(\omega) = \left(G(\omega)\right)^4 = \exp\left(-2\omega^2\right) \quad (8)$$

The templates B_4, A_4 are obtained by convolution: $B_4 = B_1 * B_1 * B_1 * B_1$; $A_4 = A_1 * A_1 * A_1 * A_1$ and result of size 1×9. The only separable 2D filter function that also has the property of circular symmetry is the Gaussian:

$$\begin{aligned} G(\omega_1,\omega_2) &= \exp\left(-\sigma^2(\omega_1^2+\omega_2^2)/2\right) \\ &= \exp\left(-\sigma^2\omega_1^2/2\right)\cdot\exp\left(-\sigma^2\omega_2^2/2\right) = G_1(\omega_1)\cdot G_2(\omega_2) \end{aligned} \quad (9)$$

We can obtain the filter templates of the Gaussian filter as an outer product of the 1D templates: $B = B_4^T \otimes B_4$ and $A = A_4^T \otimes A_4$ and they will be of size 9×9. Here the symbol $\otimes$ stands for outer product and B_4^T and A_4^T are transpose column vectors. In Fig.5(a) this 2D LP circular filter is shown.

It may be useful to distinguish between the finest capillaries, developed in the pathological process, and the larger blood vessels usually present in a normal retina, like arteries. This task could be approached in two steps; first a low-pass filtering would be useful to perform an image smoothing, rendering the finer details almost invisible; these details are smoothed out for instance by Gaussian blurring, while details like larger blood vessels will remain visible; after this pre-filtering, a simple threshold can be applied, resulting in a binary image in which larger blood vessels or other larger details are visible. The original grayscale retina image in Fig.1(a) is low-pass filtered using a Gaussian filter with $\sigma = 4$, resulting in the blurred image in Fig.5(b), in which the finer details like thin capillaries are no longer visible.

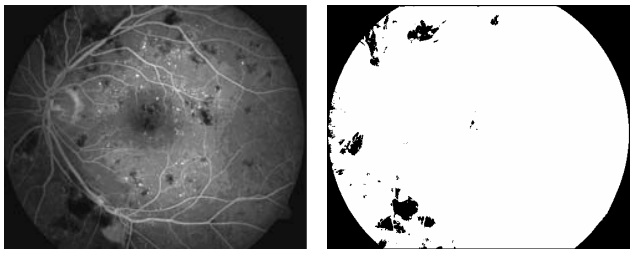

(a) (b)

Fig. 3. (a) Retina angiography; (b) Detected hemorrhage spots

(a) (b) (c) (d) (e)

Fig. 4. Types of junctions: (a), (b) – Y junctions; (c) T-junction; (d) crossing junction; (e) Original grayscale retina image with marked vessel junctions

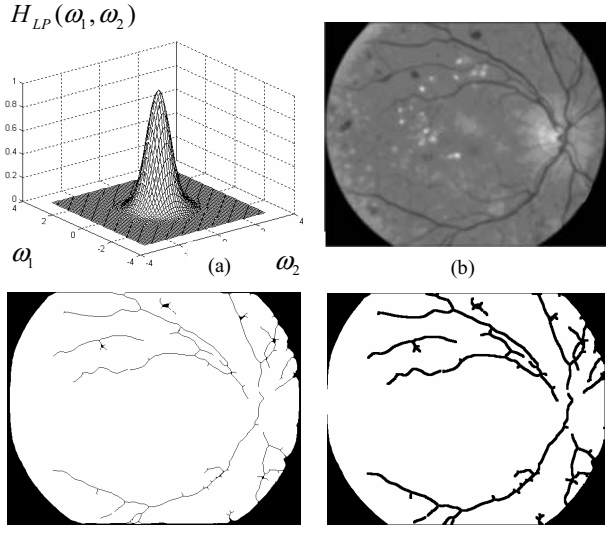

Fig. 5. (a) Frequency response of 2D Gaussian IIR filter $G_4(\omega_1,\omega_2)$; (b) blurred retina image; (c) skeletonized image; (d) dilated image

Applying a proper threshold value ($th = 0.56$), a binary image is obtained. To this image a skeletonization task is applied, then a small object removal, resulting in the image in Fig.5(c). Finally, to this image a dilation may be applied, rendering the main blood vessels visible (Fig. 5(d)).

C. Edge Detection and Small Object Removal for Blood Vessel Extraction

Blood vessels can also be put in evidence through edge detection, performed directly on the grayscale image. Image brightness and contrast may be adjusted for optimum results. This task can be accomplished using a nonlinear analog algorithm implemented on CNN. The templates are:

$$A = \begin{bmatrix} 0 & 0 & 0 \\ 0 & 2 & 0 \\ 0 & 0 & 0 \end{bmatrix};\ B = \begin{bmatrix} a & a & a \\ a & 0 & a \\ a & a & a \end{bmatrix};\ I = 0.7$$

where the parameter a is defined by a piece-wise constant function [6].The static grayscale image **P** is both applied at the input and loaded as initial state: **U(t)=P**, **X**(0)=**P**. The original image **P** is the angiography given in Fig.3(a). The resulted image after applying edge detection operator is shown in Fig.6(a) and it contains many small size "artifacts"; these in turn can be removed using the *small object remover*, used also in the previous task. This is defined by the following parameters:

$$A = \begin{bmatrix} 1 & 1 & 1 \\ 1 & 2 & 1 \\ 1 & 1 & 1 \end{bmatrix};\ B = \begin{bmatrix} 0 & 0 & 0 \\ 0 & 0 & 0 \\ 0 & 0 & 0 \end{bmatrix};\ I = 0$$

The resulted image given in Fig.6(b) is an accurate vessel map, and it can be further processed using other operators.

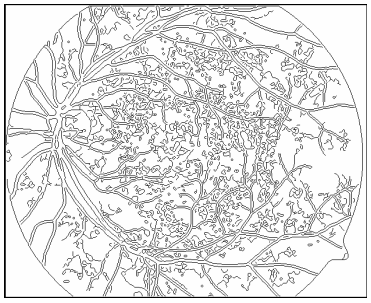

(a)

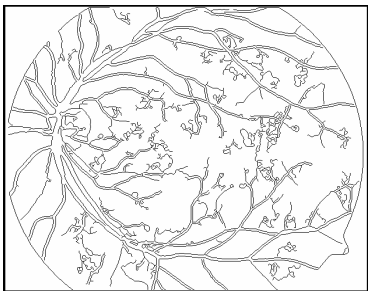

(b)

Fig. 6. Images obtained after: (a) edge detection; (b) small object removal

III. Conclusion

Some analog algorithms were discussed, which may find applications in biomedical image processing, specifically in retinal images which may present pathological aspects caused by diabetes, generally referred to as retinopathy. These tasks are easily implemented in cellular neural network systems using minimum size templates, mainly linear. Due to the parallel processing performed by the array structure, the algorithms are fast and can be grouped in analog subroutines; the template parameters are adjusted digitally. The advantage of these systems is that no analog-digital image conversions are necessary, the processing is entirely done in the analog domain, but under digital control, which ensures precision and robustness. Several analog processing tasks were presented, including morphological operations, linear filtering, thresholding etc., some proposed by the authors. These can be used as a pre-processing step in a more elaborate assisted diagnosis system, which may assess the presence of specific retinal lesions of diabetic origin. Here only a few such tasks were discussed, but the applicability of analog processing tasks is much larger.

References

[1] O. P. van Bijsterveld, *Diabetic Retinopathy*, Informa Healthcare, 2000.
[2] K. A. Neely et al., *Diabetic retinopathy*, Medical Clinics of North America, 82(4): 847–876
[3] L.O.Chua, L.Yang, "Cellular Neural Networks: Theory", *IEEE Trans. on Circuits and Systems (CAS-I)*, Vol.35, pp.1257-1272, 1988
[4] K. R. Crounse, L.O.Chua, "Methods for Image Processing and Pattern Formation in Cellular Neural Networks: A Tutorial", *IEEE Transactions on Circuits and Systems-I*, vol.42, pp.583-601, 1995
[5] *** CNN Software Library, version 1.1 – Analogical and Neural Computing Laboratory, MTA-SZTAKI, Budapest, 2000
[6] T. Roska, L. O. Chua, "The CNN universal machine: an analogic array computer", *IEEE Trans. Circuits Systems II*, vol.40, 1993, pp.163-173
[7] T. Roska, "Cellular Neural Network Technology in Image Processing - an overview", *Proceedings of KEPAF Conf. on Image Analysis and Pattern Recognition*, 1997, pp.234
[8] C. Rekeczky, A. Ushida, T. Roska, "Analogic CNN Algorithms in Medical Imaging", *1st Symposium on Nonlinear Circuits Networks*, 1995, pp.667-672
[9] G. Liszka, T. Roska, A. Zarándy, J. Hegyesi, L. Kék, C. Rekeczky, "Mammogram analysis using CNN algorithms", *Proceedings SPIE Medical Imaging*, 1995, pp.461-470
[10] A. Zarándy, C. Rekeczky, M. Csapodi, T. Roska, "Mammogram and Echocardiogram Analysis using Cellular Neural Network Technology", *ERCIM NEWS*, 1997, pp.17-18
[11] S. Jankowski, R. Wanczuk, "Improvement of Echocardiograms by CNN Programs", *Proc. of 12 European Conference on Circuit Theory and Design*, vol. 2, 1995, pp. 995-998
[12] R. Matei, L. Goraş, "Design methods for CNN spatial filters with circular symmetry", *7-th Seminar on Neural Network Applications in Electrical Engineering*, Neurel 2004, Belgrade, Serbia
[13] D. Matei, R. Matei, "Analog Linear Filtering of Biomedical Images with Cellular Neural Networks", *Proc. of 4th European Symposium on Biomedical Engineering*, *ESBME'2004*, June 25-27, 2004, Patras, Greece
[14] R. Matei, "New Image Processing Tasks on Binary Images Using Standard CNNs", *Proc. Int. Symp. on Signals, Circuits and Systems, SCS'2001*, July 10-11, 2001, Iaşi, Romania